Check for updates

Received: 18 April 2021 | Revised: 22 December 2021 | Accepted: 1 February 2022

DOI: 10.1002/gdj3.149

Geoscience Data Journal RMetS WILEY

DATA ARTICLE

Updatable dataset revealing decade changes in land cover types in Mongolia

Juanle Wang[1,2,3] | **Haishuo Wei**[1,4] | **Kai Cheng**[1,2] | **Altansukh Ochir**[5,6] | **Yating Shao**[1,7] | **Jinyi Yao**[1,4] | **Yuxin Wu**[1,4] | **Xuehua Han**[1,2] | **Davaadorj Davaasuren**[8] | **Sonomdagva Chonokhuu**[5] | **Yezhi Zhou**[1,9] | **Min Zhang**[1,2] | **Xiaoming Cao**[10] | **Mengxu Gao**[11] | **Junxiang Zhu**[12] | **Yifan Li**[13] | **Qiong Li**[1,7] | **Xiya Liang**[1,14] | **Kai Li**[1,9]

[1]State Key Laboratory of Resources and Environmental Information System, Institute of Geographic Sciences and Natural Resources Research, Chinese Academy of Sciences, Beijing, China

[2]University of Chinese Academy of Sciences, Beijing, China

[3]Jiangsu Center for Collaborative Innovation in Geographical Information Resource Development and Application, Nanjing, China

[4]School of Civil and Architectural Engineering, Shandong University of Technology, Zibo, China

[5]School of Engineering and Applied Sciences, National University of Mongolia, Ulaanbaatar, Mongolia

[6]Institute for Sustainable Development, National University of Mongolia, Ulaanbaatar, Mongolia

[7]School of Marine Technology and Geomatics, Jiangsu Ocean University, Jiangsu, China

[8]School of the Art & Sciences, National University of Mongolia, Ulaanbaatar, Mongolia

[9]College of Geoscience and Surveying Engineering, China University of Mining & Technology (Beijing), Beijing, China

[10]Institute of desertification, Chinese Academy of Forestry Sciences, Beijing, China

[11]National Science and Technology Infrastructure Center, Ministry of Science and Technology of the People's Republic of China, Beijing, China

[12]Australasian Joint Research Centre for Building Information Modeling, School of Built Environment, Curtin University, Bentley, Western Australia, Australia

[13]The Institute of Oceanology, Chinese Academy of Sciences, Qingdao, China

[14]College of Geomatics, Xi'an University of Science and Technology, Xian, China

Dataset

Identifier: https://doi.org/10.6084/m9.figshare.14390912.v1

Creator: Juanle Wang, Haishuo Wei, Kai Cheng, Yating Shao, Jinyi Yao, Yuxin Wu, Xuehua Han, Altansukh Ochir, Davaadorj Davaasuren, Sonomdagva Chonokhuu, Yezhi Zhou, Min Zhang, Xiaoming Cao, Mengxu Gao, Junxiang Zhu, Yifan Li

Dataset correspondence: wangjl@igsnrr.ac.cn

Title: An updatable dataset revealing decade changes in land cover types in Mongolia

Publisher: figshare

Publication year: 2021

Resource type: Raster files

Version: V1

Conflicts of interests: The authors declare that they have no conflict of interest.

This is an open access article under the terms of the Creative Commons Attribution License, which permits use, distribution and reproduction in any medium, provided the original work is properly cited.
© 2022 The Authors. *Geoscience Data Journal* published by Royal Meteorological Society and John Wiley & Sons Ltd.

20496060, 2022, 2, Downloaded from https://rmets.onlinelibrary.wiley.com/doi/10.1002/gdj3.149 by Curtin University Library, Wiley Online Library on [06/02/2023]. See the Terms and Conditions (https://onlinelibrary.wiley.com/terms-and-conditions) on Wiley Online Library for rules of use; OA articles are governed by the applicable Creative Commons License

Correspondence
Juanle Wang, State Key Laboratory of Resources and Environmental Information System, Institute of Geographical Sciences and Natural Resources Research, Chinese Academy of Sciences, 11A, Datun Road, Chaoyang District, Beijing 100101, China.
Email: wangjl@igsnrr.ac.cn

Funding information
This article was funded by the National Nature Science Foundation of China [grant number 41971385], the Strategic Priority Research Program (Class A) of the Chinese Academy of Sciences [grant numbers XDA2003020302], the fund programme of the Asia Research Center, Mongolia and Korea Foundation for Advanced Studies [grant number P2018-3606], and the Construction Project of the China Knowledge Center for Engineering Sciences and Technology [grant number CKCEST-2020-2-4].

Abstract

The Mongolian Plateau (MP) is in the interior of Northeast Asia, far from the sea, and is extremely vulnerable to climate change and the deleterious effects of human activity. The United Nations Sustainable Development Goals (SDGs) explicitly set land degradation neutrality (LDN) as one of the sub-goals of the seventeen main tasks. However, achieving this goal in Mongolia, a country with a fragile and sensitive ecological environment and a lack of high-precision land cover and land degradation monitoring data, is challenging. In this study, we established rules for remote sensing-based land cover classification and reference threshold ranges based on an object-oriented remote sensing interpretation method. Then, we obtained the refined land cover data of Mongolia from 1990, 2000, 2010 and 2020 with 30-m resolution. The land cover classification of Mongolia comprises 11 categories: forest, meadow steppe, real steppe, desert steppe, barren, sand, desert, ice, water, cropland and built area. The overall classification accuracies, corresponding to the aforementioned data year, were 82.26%, 82.77%, 92.34% and 81.84%, respectively. We found that the land cover showed an apparent law of zonal gradual change. Among them, barren land, real steppe, desert steppe and forest were consistently the four major land cover types. Since the last 30 years, barren land areas present an overall decreasing trend, showing a trend of shrinking to the south. Overall, real steppe presents a wavelike decreasing trend, and desert steppe shows a fluctuating increasing trend. The forest area is relatively stable with no notable changes in spatial distribution. The dataset of this study fills the gaps in high-resolution land cover data for Mongolia, and it can provide fundamental scientific data to support sustainable development in the MP.

1 | INTRODUCTION

The Mongolian Plateau (MP) lies in the hinterlands of Northeast Asia, within the transition area between the arid and semi-arid climate zones. A climate distribution pattern is formed here with the semi-humid zones in the north and east and the semi-arid, arid and extremely arid zones in the southwest; this distribution has created remarkable features of vegetation cover and gradient changes. Grassland resources are abundant in Mongolia. However, drought, land degradation and extreme weather involving sand and dust occur frequently (Uno et al., 2006; Zhang et al., 2003). The ecosystem status and changes in the MP have an important impact on the ecological security, regional resources and environmental sustainability of Northeast Asia (Bao et al., 2013; Yue et al., 2011; Zhang, 2016).

Due to the combined influence of climate change and human activity, land cover changes have accelerated land degradation in general. According to data released by the Ministry of Natural Environment and Tourism of Mongolia in 2017, 76.8% of Mongolia's land has experienced desertification to some degree: 24.1% of the land area has experienced slight desertification, 29.8% moderate, 16.8% severe and 6.1% heavily degraded. Desertification continues to spread to other areas at a faster rate, including to lush grassland areas such as Dornod and Hentiy (Asigang, 2017). In 2015, the United Nations Sustainable Development Goals (SDGs) explicitly set land degradation neutrality (LDN) as one of the sub-goals of the fifteenth main task. Refined multi-decadal fundamental land cover data products are urgently needed by decision makers responsible for the sustainable development of the MP. Currently, there are several sets of global scale land cover data covering Mongolia, such as the IGBP-DIScover from the United States Geological Survey (USGS); land cover data for 1998 from the University of Maryland; global land cover database for 2000 from the European Commission's Joint Research Centre; land cover data from Moderate-Resolution Imaging Spectroradiometer (MODIS), which are updated quarterly; and GlobCover from the European Space Agency (ESA). Researchers can extract land cover

20496060, 2022, 2, Downloaded from https://rmets.onlinelibrary.wiley.com/doi/10.1002/gdj3.149 by Curtin University Library, Wiley Online Library on [06/02/2023]. See the Terms and Conditions (https://onlinelibrary.wiley.com/terms-and-conditions) on Wiley Online Library for rules of use; OA articles are governed by the applicable Creative Commons License

data of Mongolia using these datasets. However, the spatial and temporal resolutions of these datasets are very low in the MP, and there are significant differences among the classification systems and their accuracies (Tian et al., 2014).

In recent years, there has been an increase in research on land cover interpretation and land cover change analysis in Mongolia and the entire MP using various large-scale remote sensing data sources. Based on ESA 300-m resolution land cover data from 1970 to 2005, Shi et al. (2013) completed land cover maps and dynamic change maps of the MP using human–computer interactive interpretation. Using MODIS land cover data from 2005 to 2015 with 500-m resolution, Zhang et al. (2019) conducted a land cover change analysis and ecological carrying capacity assessment in Mongolia. Based on the ESA land cover datasets, Zhou et al. (2014) modified the 250-m resolution land cover data of the MP for 1980 and 2006. Despite the increase in temporal resolution, land cover datasets covering Mongolia still have coarse spatial resolution, and no continuous datasets have been updated across decades.

With the enrichment of remote sensing data sources, some researchers have begun to use medium- and high-resolution images to obtain regional land cover maps of Mongolia. By using Landsat Thematic Mapper (TM) images, which have a 30-m resolution, as the basic data source, Tian et al. (2014) adopted the decision tree method of Quick Unbiased and Efficient Statistical Tree (QUEST) and visual interpretation to obtain the land cover data for Tov and Ulaanbaatar for 2010. Based on remote sensing images of the Landsat series, Buyan-Erdene et al. (2019) analysed land cover changes in the Mongolia Uvs Lake Basin from 1995 to 2015. Lamchin et al. (2016) developed a quantitative assessment method, using data from Landsat TM and Enhanced Thematic Mapper (ETM+) for land cover changes in the Hogno Khaan Nature Reserve. However, these studies obtained land cover data for a specific geographical unit or provincial district in Mongolia and did not cover all of Mongolia. In 2014, China released GlobeLand30, a globe land cover dataset with a 30-m resolution (Chen et al., 2015). This dataset contains 10 major land cover types, but there is no classification of grassland sub-types. Thus, this dataset has limitations in the Mongolian Plateau, where grasslands are widely distributed, but there are diverse the grassland types. Data product availability remains a significant challenge.

To address the problem of fine extraction of Mongolian land cover, based on the object-oriented remote sensing classification method and setting multi-rules and multi-thresholds, the classification of land cover data of 1990, 2000, 2010 and 2020 at 30-m resolution was accomplished for the first time. Furthermore, according to the characteristics of vegetation cover in Mongolia, this dataset distinguished various grassland types in detail. In the object-oriented remote sensing classification method, remote sensing images are segmented, and pixels with the same characteristics are formed into a homogeneous object. Then, the object is used to replace the pixel as the basic unit of image classification (Baltsavias, 2004). In this way, the shapes of many kinds of ground objects can be defined in classification results, individual locations can be completely mapped, and the salt-and-pepper image noise resulting from poorly defined pixels can be effectively avoided (Hu et al., 2012). After image segmentation and object construction, classification rules and reference thresholds must be established manually. Compared with the current supervised classifiers methods (maximum likelihoods, support vector machines, etc.), this method requires a strict process, stepwise procedure in the implementation stage. These refined data products are expected to provide fundamental support for natural resource management, climate change adaption and regional sustainable development decision-making in the MP.

2 | STUDY AREA AND DATA

2.1 | Study area

Mongolia is located between 42°N, 88°E and 52°N, 120°E, with an area of approximately 1,566,500 km^2. The overall altitude of Mongolia is high, and it rises progressively from east to west. The terrain primarily consists high plains. Most areas of Mongolia have a continental temperate grassland climate (Batjargal, 1997; Zhuo, 2007). The annual average precipitation is approximately 120–250 mm and 70% of this precipitation occurs between July and August. Mongolian vegetation consists of Siberian coniferous forests in the north, the Central Asian steppe, and desert steppe in the south (Unurbaatar et al., 2014; Wang, Cheng, et al., 2019; Wei et al., 2008).

2.2 | Data sources

Landsat TM, ETM+ and Operational Land Imager (OLI) images with 30-m resolution were the basic remote sensing data used in this study. Images having cloud cover less than 5% were selected from June to September in 1990, 2000, 2010 and 2020. A total of 528 Landsat series remote sensing images were used, including 132 Landsat TM images, 264 Landsat ETM+ images and 132 Landsat OLI images. All images were obtained from the USGS website (http://earthexplorer.usgs.gov/).

Auxiliary data include: (1) digital elevation model (DEM) data from the Advanced Spaceborne Thermal

20496060, 2022, 2, Downloaded from https://rmets.onlinelibrary.wiley.com/doi/10.1002/gdj3.149 by Curtin University Library, Wiley Online Library on [06/02/2023]. See the Terms and Conditions (https://onlinelibrary.wiley.com/terms-and-conditions) on Wiley Online Library for rules of use; OA articles are governed by the applicable Creative Commons License

Emission and Reflection Radiometer (ASTER) Global Digital Elevation Model (GDEM) (http://gdem.ersdac.jspacesystems.or.jp/); (2) temperature, precipitation, socioeconomic and other statistical data from the statistical data service website for Mongolia (http://www.1212.mn); and (3) field investigation data of Mongolia.

3 | METHODS

3.1 | Land cover classification system of Mongolia

A remote sensing land cover classification system was established based on the land cover conditions in Mongolia. The first level of land cover classification for Mongolia contained forest, grassland, barren, ice, water, cropland and built area. Based on the vegetation coverage, the grassland type was subdivided into desert steppe, real steppe and meadow steppe. Their internal criteria were: 'vegetation coverage >30%', '10% < vegetation coverage < 30%' and '5% < vegetation coverage < 10%' (Wang et al., 2018). Based on the differences in soil or stone quality of barren land, it was further divided into two secondary categories: sand and barren. Cumulatively, 11 categories of land cover types were defined: forest, meadow steppe, real steppe, desert steppe, barren, sand, desert, ice, water, cropland and built area (as shown in Table 1).

3.2 | Data preprocessing

Multiple steps were required to pre-process the data in this study. First, selected images were pre-processed, including radiometric and atmospheric correction. Radiometric correction is the process of eliminating all types of distortions in the image data. The radiometric calibration module in the Environment for Visualizing Images (ENVI) 5.1 was used to achieve radiometric correction. Atmospheric correction is the process of eliminating radiometric error caused by atmospheric influences and retrieving the true surface reflectance of ground objects (Zheng & Zeng, 2004). This was completed using the FLASSH module in ENVI 5.1. Prior to atmospheric correction, the sensor type, ground elevation, image generation time, atmospheric model parameters and results of radiometric correction were successively entered in the module. Finally, using the vector data from the Mongolian administrative division, the remote sensing images were clipped and mosaicked to synthesize an image map covering the entire study area.

3.3 | Remote sensing interpretation

(1) Multiscale segmentation

Remote sensing interpretation was performed using eCognition. Multiscale segmentation is the first step in image classification processing. It is used to divide a raster image into several objects according to certain rules, and these objects become the smallest objects to be processed (Ma et al., 2015). First, we selected the 'multi-resolution segmentation' algorithm and set the appropriate value of segmentation scale to complete remote sensing image segmentation. Then, we chose the 'spectral difference segmentation' algorithm, set the maximum spectral difference value, and finally, completed the segmentation of spectral difference.

(2)Classification of land cover types

1) Classification of water. The reflectance of water in the near-infrared band is low, and it often shows a dark tone in images (Gao, 1996; Wang, Wei, et al., 2019). Therefore, we used the normalized difference water index (NDWI) to extract information about water. The NDWI calculation formula is shown in Equation 1. Setting the corresponding threshold of NDWI can effectively suppress vegetation information and emphasize water information. Objects with NDWI greater than 0.036 were classified as water (as shown in Table 2).

$$\mathrm{NDWI} = (G - \mathrm{NIR})/(G + \mathrm{NIR}), \quad (1)$$

where G and NIR are the green and near-infrared bands, respectively.

2) Classification of clouds and shadows. Although the cloud cover in each remote sensing image we selected was less than 5%, there were still clouds and shadows in some images, affecting the accuracy of the final classification results. We separated the clouds and shadows as independent 'land cover types' and replaced them with the actual land cover types. Experiments showed that when the NDWI value is negative, most of the clouds and shadows could be separated. Therefore, by setting the appropriate NDWI thresholds, cloud and shadow information can be extracted effectively.

3) Classification of vegetation. The normalized difference vegetation index (NDVI) is a common tool used to extract vegetation information (Cao et al., 2016; Ren et al., 2017). We classified the objects with NDVI values greater than 0.1 as vegetation. The equation for calculating NDVI is as follows:

$$\mathrm{NDVI} = (\mathrm{NIR} - R)/(\mathrm{NIR} + R) \quad (2)$$

20496060, 2022, 2, Downloaded from https://rmets.onlinelibrary.wiley.com/doi/10.1002/gdj3.149 by Curtin University Library, Wiley Online Library on [06/02/2023]. See the Terms and Conditions (https://onlinelibrary.wiley.com/terms-and-conditions) on Wiley Online Library for rules of use; OA articles are governed by the applicable Creative Commons License

TABLE 1 Land cover classification system in Mongolia

Land cover types	Landscape images	Land cover types	Landscape images
Forest		Meadow steppe	
Real steppe		Desert steppe	
Cropland		Water	
Built area	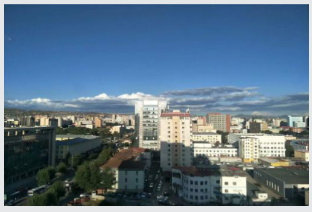	Desert	
Sand	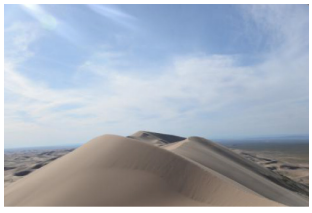	Barren land	

where R is the red band.

We used various threshold values of NDVI and other parameters to classify land covers as forest, desert steppe, real steppe and meadow steppe within the vegetation category. As the canopy densities of forest are greater than 30%, their vegetation coverage is higher, and the NDVI value is relatively high. We classified objects in the vegetation category as forests when their NDVI values are greater than 0.5 (as shown in Table 2). Desert steppe is grassland dominated by strong xerophytes, and the vegetation coverage is the lowest among vegetation types, and the corresponding NDVI value is relatively small. By experimenting, we classified the objects in the vegetation category with NDVI values between 0.1 and 0.2 as desert steppe. The real steppe is grassland dominated by xerophytes, whose vegetation coverage is slightly higher than that of desert steppe. We classified the objects in the vegetation category with $0.2 \leq \text{NDVI} < 0.4$ as real steppe. In general, meadow steppe is mostly distributed along rivers, lakes and other water sources. Its vegetation coverage was also the highest among all grassland types in this study. We classified objects in the vegetation category with NDVI values between 0.4 and 0.5 and the values of distance to water less than 40 pixels as meadow steppe (as shown in Table 2).

4) Classification of cropland. Because the distribution of cropland is relatively concentrated and the shapes are regular, the 'compactness' parameter is selected to extract the cropland information. We classified objects with compactness values less than or equal to 1.4 as cropland (as shown in Table 2).

5) Classification of built area. Mongolia is a sparsely populated country with a large population concentrated in the capital of Ulaanbaatar, provincial capitals and areas rich in natural resources. We achieved effective extraction

20496060, 2022, 2, Downloaded from https://rmets.onlinelibrary.wiley.com/doi/10.1002/gdj3.149 by Curtin University Library, Wiley Online Library on [06/02/2023]. See the Terms and Conditions (https://onlinelibrary.wiley.com/terms-and-conditions) on Wiley Online Library for rules of use; OA articles are governed by the applicable Creative Commons License

TABLE 2 Interpretation rules and reference thresholds used in land cover classification

Land cover types	Rules and reference threshold
Forest	NDVI > 0.5
Meadow steppe	0.4 ≤ NDVI < 0.5; Distance to water < 40 pixels
Real steppe	0.2 ≤ NDVI < 0.4
Desert steppe	0.1 < NDVI < 0.2
Barren lands	NDSI > 0.03
Desert	visual interpretation
Sand	Blue + Green + Red + NIR + SWIR1 + SWIR2 ≥ 600
Cropland	Compactness ≤ 1.4
Built area	visual interpretation
Ice	visual interpretation
Water	NDWI > 0.036

of built area information through visual interpretation and manual modification.

6) Classification of barren land. In the non-vegetated areas, high reflection is observed in the red band and low reflection in the green band. Therefore, information on barren land could be obtained using the normalized difference soil index (NDSI) (Kearney et al., 1995). We classified objects with NDSI values greater than 0.03 as barren land (as shown in Table 2). The equation for NDSI is as follows:

$$\mathrm{NDSI} = (\mathrm{MIR} - \mathrm{NIR})/(\mathrm{MIR} + \mathrm{NIR}) \quad (3)$$

where MIR represents the mid-infrared band.

7) Classification of sand. Sand is generally distributed in areas with vegetation coverage below 5%. Owing to the low vegetation coverage and high reflectivity of the ground objects, sand generally appears as bright colours in remote sensing images. Therefore, 'Brightness' parameters are generally used in the extraction of sand information (Wang, Wei, et al., 2019). We classified objects as sand when the sum of the blue, green, red, NIR, SWIR1 and SWIR2 bands is equal or greater than 600 (as shown in Table 2).

8) Classification of desert. Desert areas are generally fixed and have continuous large areas. We used Google Maps for visual interpretation and then performed manual modification.

9) Classification of ice. The snow- and ice-covered areas are relatively small and mostly distributed in high-altitude mountains. We adopted visual interpretation with a man-computer interactive method to retrieve them.

(3)Manual modification

The automatic computational classification inevitably produces mixed, incorrect and unclassified objects. Therefore, all classified objects must be visually confirmed and any misclassified objects manually corrected.

(4)Smoothing and merging

After image classification, examination and modification, image smoothing is often needed to make the classification results more reasonable. We chose to use the growing and shrinking algorithm for processing. However, smoothing can cause narrow rivers to be incorporated into their adjacent land cover types. Then, the phenomenon of river discontinuity will occur in the land cover distribution map. To avoid this mistake, we selected 'water' in the 'Class filter' option of the 'growing and shrinking' algorithm.

To reduce the degree of fragmentation of the classification results, we used the 'remove objects' algorithm to combine objects with relatively small areas. Then, we used the 'merge region' algorithm to combine objects belonging to the same land cover type into a large object. Finally, we converted the obtained data into output to produce the corresponding land cover classification map.

The above threshold information in Table 2 is the reference threshold. Due to the difference in the acquisition time and the acquisition angle of remote sensing images, the scene and noise are different. Therefore, the thresholds of different scene regions need to be determined separately.

3.4 | Precision evaluation

In total, 1654 sample points were collected. Among them, we selected 429 points representing various land cover types for field verification. From the Degree Confluence Program (DCP, http://www.confluence.org/), we collected 512 latitude and longitude crossing points. Furthermore, 713 verification points with high resolution were collected from Google Earth. Since 2013, our research team has conducted 10 field trips to Mongolia. During the field trips, we determined the latitude and longitude coordinates of the verification points using hand-held GPS and verified the land cover type visually or based on prior knowledge. To maintain the uniform distribution of verification points and make them more representative, we set one verification point every 40 km in the field investigation route. For high-resolution images from Google Earth, we determined the coordinates of the verification points and classified the

20496060, 2022, 2, Downloaded from https://rmets.onlinelibrary.wiley.com/doi/10.1002/gdj3.149 by Curtin University Library, Wiley Online Library on [06/02/2023]. See the Terms and Conditions (https://onlinelibrary.wiley.com/terms-and-conditions) on Wiley Online Library for rules of use; OA articles are governed by the applicable Creative Commons License

corresponding land cover types using Google satellite images. For verification points from DCP and Google Earth, we applied an approximately uniform distribution covering all of Mongolia. Based on the above data, confounding matrices (Green, 2009) were constructed for different years. We then acquired producer, user and overall classification accuracy (Foody, 2002; Mengistie et al., 2013).

4 | RESULTS

4.1 | Land cover distribution pattern and its change

Figure 1 shows the latest land cover data of Mongolia (2020) as an example of land cover distribution. The area under each land cover type and the percentage of the total area of Mongolia covered by each of them are shown in Table 3. The area change curves of different land cover types are shown in Figure 2.

In the past 30 years, barren land, real steppe, desert steppe and forest have consistently remained the four major land cover types. Barren land in Mongolia has experienced a process of 'decreasing–increasing–greatly decreasing' area. In other words, the area under barren land, as a whole, presents a decreasing trend. According to the characteristics of vegetation coverage, we divided grasslands into three types: desert steppe, real steppe and meadow steppe. Most of the grasslands is real steppe or desert steppe. The meadow steppe area is small, covering less than 2% of the total area of Mongolia. From Table 3, we can find that real steppe is always the largest area of grassland type. In 1990, real steppe is principally in northern and central Mongolia. It accounts for 26.42% of Mongolia's overall land area. In 2000, real steppe is chiefly in northeastern Mongolia, north of Arhangay and Bayanhongor, accounting for approximately 29.04% of Mongolia's overall land area. It shows a significant increase in area from 1990. In 2010, real steppe is principally in the north and northeast of Mongolia, accounting for approximately 24.67% of the total land area. Compared with 2000, the area of real steppe decreased. In 2020, real steppe is principally in northern Mongolia and accounted for approximately 27.56% of the total land area. Thus, real steppe in Mongolia have experienced a process of 'increasing–decreasing–increasing' area. Overall, real steppe presents

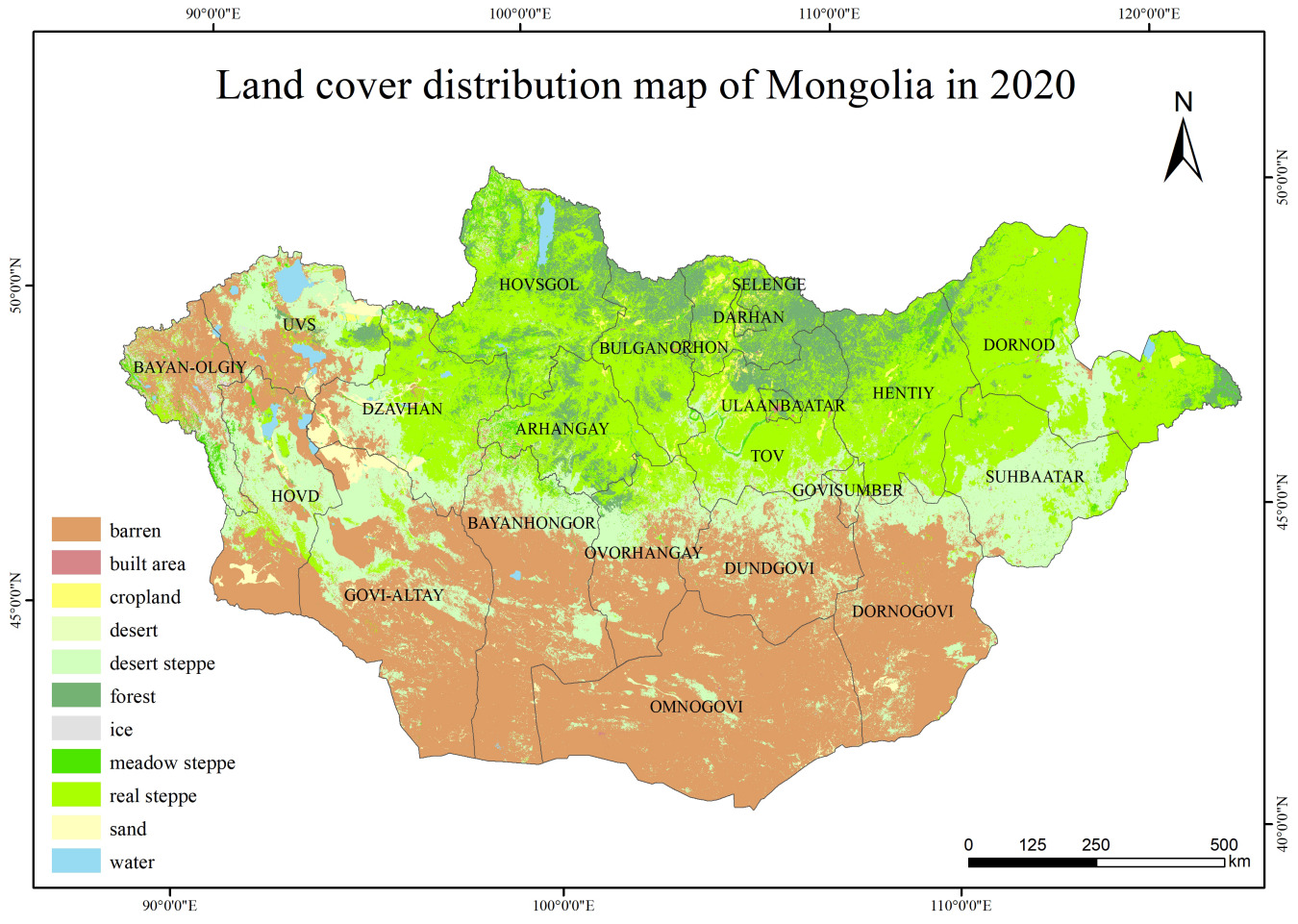

FIGURE 1 Land cover distribution map of Mongolia in 2020

20496060, 2022, 2, Downloaded from https://rmets.onlinelibrary.wiley.com/doi/10.1002/gdj3.149 by Curtin University Library, Wiley Online Library on [06/02/2023]. See the Terms and Conditions (https://onlinelibrary.wiley.com/terms-and-conditions) on Wiley Online Library for rules of use; OA articles are governed by the applicable Creative Commons License

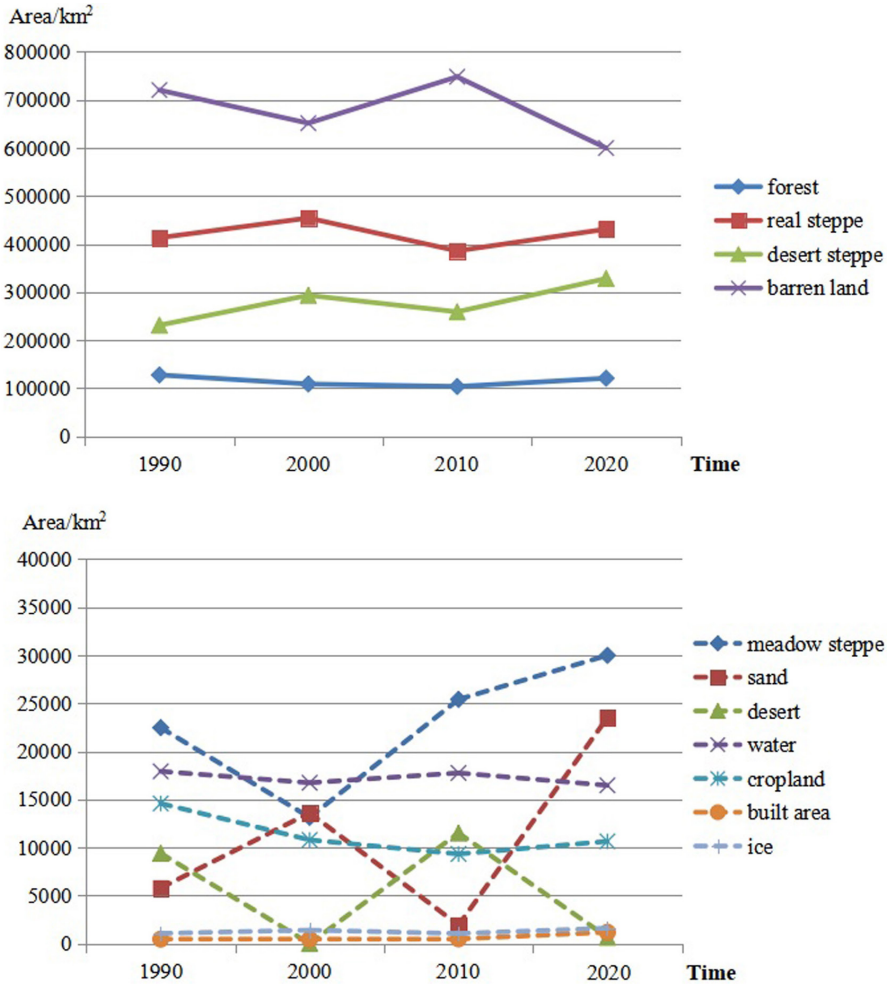

FIGURE 2 Change in area of various land cover types in Mongolia

a slight increasing trend. Desert steppe is mainly in north-western, central and north-eastern Mongolia in 1990, accounting for 14.78% of Mongolia's overall area. In 2000, desert steppe is principally in north-western Mongolia in isolated blocks and in central and northern Mongolia in continuous blocks. Compared with 1990, the area under desert steppe increased in 2000. In 2010, desert steppe is principally in western Mongolia in the form of belts, and it is concentrated in central and north-eastern Mongolia in the form of blocks. The coverage of desert steppe had decreased since 2000. In 2020, desert steppe is mainly in north-western and central Mongolia, accounting for 20.99% of Mongolia's overall area. In the past 30 years, the area under desert steppe in Mongolia has demonstrated an 'increasing–decreasing–slightly increasing' trend. Overall, the area under desert steppe shows a fluctuating increasing trend. It has also shown a trend of continuous northward expansion from the south.

Overall, the area under grasslands in Mongolia has shown a fluctuating and slightly increasing trend in the past 30 years. This may be chiefly related to climate change. The melting of some of the ice and snow, as the global climate warms, brings relatively abundant water resources to some river valleys and lower elevations, which in turn promotes the growth of vegetation and leads to an increase in grasslands. Alternatively, the East Asian Monsoon reaches Mongolia's eastern margin, bringing substantial precipitation to north-eastern Mongolia (Wang et al., 2020) and promoting the growth of vegetation. There has been insignificant change in the spatial distribution of forest over the past 30 years. However, the area of forest in Mongolia has declined slightly. Since the 1990s, Mongolia's economic policy has gradually changed from one of only trading timber with Russia (Bayarkhuu, 2013). Its timber trade with other countries has gradually increased. With the continuous development of the timber industry, human logging activities have increased, resulting in a continual decrease in forest area. The built area showed an increasing trend. The city population of Mongolia grew by approximately 1 million from 1990 to 2019 (National Statistics Office of Mongolia, 2020). The rate of increase is approximately 84.17%. This significant increase in urban population has accelerated the growth of built area. The coverage of cropland has been continuously decreasing. In the early 1990s, the fundamental social and economic system of Mongolia underwent drastic

20496060, 2022, 2, Downloaded from https://rmets.onlinelibrary.wiley.com/doi/10.1002/gdj3.149 by Curtin University Library, Wiley Online Library on [06/02/2023]. See the Terms and Conditions (https://onlinelibrary.wiley.com/terms-and-conditions) on Wiley Online Library for rules of use; OA articles are governed by the applicable Creative Commons License

TABLE 3 Areas and proportions of different land cover types in different years

Year	Land cover type	Area (km^2)	Ratio (%)	Year	Land cover type	Area (km^2)	Ratio (%)
1990	Forest	127,739.50	8.17	2000	Forest	108,885.11	6.96
	Meadow steppe	22,469.75	1.44		Meadow steppe	13,141.31	0.84
	Real steppe	413,244.70	26.42		Real steppe	454,313.75	29.04
	Desert steppe	231,261.50	14.78		Desert steppe	293,489.19	18.76
	Barren lands	720,463.70	46.06		Barren lands	651,589.80	41.65
	Sand	5798.05	0.37		Sand	13,610.64	0.87
	Desert	9403.51	0.60		Desert	10.95	0.0007
	Water	17,931.03	1.14		Water	16,739.52	1.07
	Cropland	14,587.19	0.93		Cropland	10,794.64	0.69
	Built area	473.29	0.03		Built area	469.33	0.03
	Ice	1069.07	0.07		Ice	1408.00	0.09
	Total	1,564,441.29	100		Total	1,564,441.29	100
2010	Forest	103,668.07	6.63	2020	Forest	120,888.40	7.73
	Meadow steppe	25,413.07	1.62		Meadow steppe	29,994.30	1.92
	Real steppe	385,907.27	24.67		Real steppe	431,160.13	27.56
	Desert steppe	259,077.15	16.56		Desert steppe	328,400.07	20.99
	Barren lands	748,184.75	47.83		Barren lands	599,908.33	38.35
	Sand	1929.89	0.12		Sand	23,517.10	1.50
	Desert	11,513.77	0.74		Desert	663.02	0.04
	Water	17,762.55	1.14		Water	16,469.79	1.05
	Cropland	9330.58	0.60		Cropland	10,645.06	0.68
	Built area	495.89	0.03		Built area	1186.57	0.08
	Ice	1058.31	0.07		Ice	1608.52	0.10
	Total	1,564,441.29	100		Total	1,564,441.29	100

changes (Wei, 2015). Under the influence of a market economy, profits from cropland have decreased, leading more people to give up farming. Meanwhile, the promulgation of a series of laws and policies, such as the policy of 'Civil Freedom' in the choice of residence and the 'Law on Allocation of Land to Mongolian Citizens for Ownership' increased the speed of cropland change and transfer in Mongolia (Buren, 2011; Dai, 2013). These are the main causes of cropland reduction.

4.2 | Accuracy of results

The distribution of the land cover data verification points in different years is shown in Figure 3. Table 4 shows the confusion matrices of the land cover data in different years. Table 5 shows the producer accuracies, user accuracies, omission errors and commission errors of the obtained land cover data for different years. The overall classification accuracies of land cover data in 1990, 2000, 2010 and 2020 were 84.19%, 82.12%, 81.84% and 81.84%, respectively. The Kappa coefficients of land cover data in 1990, 2000, 2010, and 2020 were 0.8052, 0.7656, 0.7985 and 0.7991, respectively. The data obtained in this study have greater precision and detail than the data from related studies (Tian et al., 2014; Wei et al., 2008; Zhang et al., 2019).

5 | DATA AVAILABILITY AND UNCERTAINTY

5.1 | Data availability

Land cover data of Mongolia in 1990, 2000, 2010 and 2020 can be obtained from https://figshare.com/articles/dataset/An_updatable_dataset_revealing_changes_in_land_cover_types_in_Mongolia/14390912, and its DOI is 10.6084/m9.figshare.14390912.v1 (Wang et al., 2021). The land cover data in the four phases are all raster data (.img format), with a total data volume of approximately 266 MB. The projection method of land cover data is the

20496060, 2022, 2, Downloaded from https://rmets.onlinelibrary.wiley.com/doi/10.1002/gdj3.149 by Curtin University Library, Wiley Online Library on [06/02/2023]. See the Terms and Conditions (https://onlinelibrary.wiley.com/terms-and-conditions) on Wiley Online Library for rules of use; OA articles are governed by the applicable Creative Commons License

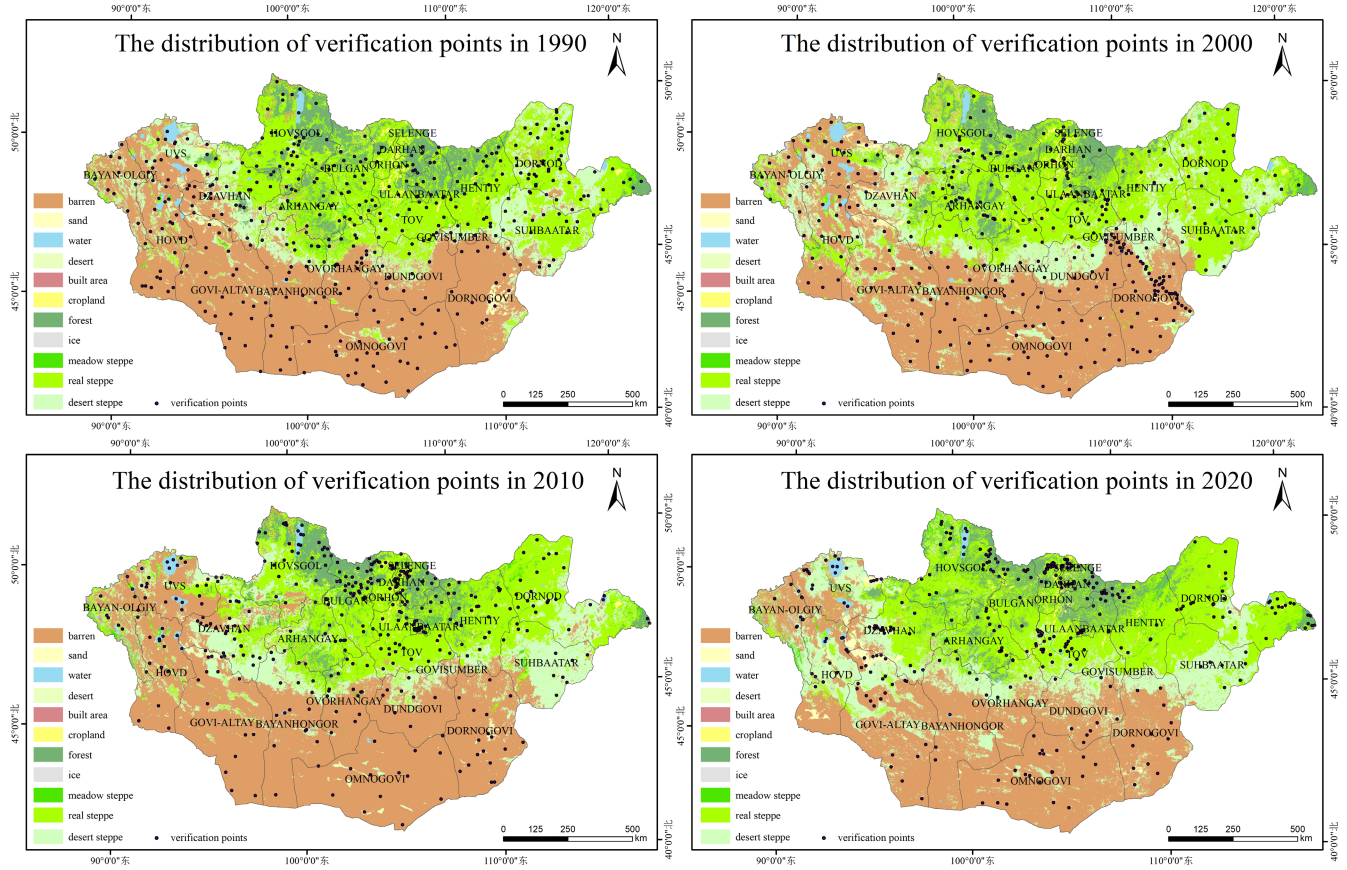

FIGURE 3 Maps showing the distribution of verification points of land cover data

Albers Equal Area Conical projection, and the spatial resolution is 30 m. The attribute value in each phase of land cover data is the code of land cover types. Among them, code 11 is forest, 21 is meadow steppe, 22 is real steppe, 23 is desert steppe, 31 is ice, 41 is cropland, 51 is water, 61 is built area, 71 is sand, 72 is barren land, and 73 is desert.

5.2 | Data uncertainty and limitations

The land cover classification system based on remote sensing images is different from other non-remote sensing classification systems in terms of definitions such as forest, grassland and barren land. To avoid confusion with different data products with different approaches, users should clearly understand these class definitions. Because the land cover data of all the four phases in this dataset are based on the same classification system and remote sensing processing method, they can be used for longitudinal comparison and directly reflect the land cover patterns and trend changes in Mongolia. This dataset also is easy to use as a national scale data product and has resolution advantages compared with other global level datasets covering Mongolia.

Although the resolution is high in this product, there are still some challenges in obtaining accurate land cover information in some transition regions, such as the transitions between barren land and desert steppe, and between desert steppe and real steppe. Grassland information in these regions is very 'weak' in spectral indices such as NDVI. Thus, more advanced technologies are needed to decrease the uncertainty in these regions.

Since 2013, our research team has made multiple field investigation trips to Mongolia and obtained annual field verification data. However, we cannot collect ground truth directly for 1990 and 2000 in this dataset. Therefore, the accuracy for that period can only be verified by searching for more DCP points and high-resolution Google Earth images close to those years. As more auxiliary data are collected, the quality of this series will be improved.

5.3 | Application potential

This dataset fills gaps in high-resolution land cover data for Mongolia. It can provide data support for the assessment of land degradation and restoration in Mongolia, the response of climate change and surface vegetation in

20496060, 2022, 2, Downloaded from https://rmets.onlinelibrary.wiley.com/doi/10.1002/gdj3.149 by Curtin University Library, Wiley Online Library on [06/02/2023]. See the Terms and Conditions (https://onlinelibrary.wiley.com/terms-and-conditions) on Wiley Online Library for rules of use; OA articles are governed by the applicable Creative Commons License

TABLE 4 Confusion matrices of the land cover data

Year	Land cover type	Forest	Meadow steppe	Real steppe	Desert steppe	Cropland	Water	Built area	Sand	Barren lands	Desert	Ice
1990	Forest	40	3	4	0	0	0	0	0	0	0	0
	Meadow steppe	0	12	1	1	0	0	0	0	0	0	0
	Real steppe	0	4	104	8	0	0	0	0	2	0	0
	Desert steppe	0	2	6	58	0	0	0	1	6	2	0
	Cropland	0	0	0	0	3	0	0	0	0	0	0
	Water	0	1	0	0	0	20	0	0	1	0	0
	Built area	0	0	2	0	1	0	5	0	0	0	0
	Sand	0	0	0	0	0	0	0	3	0	0	0
	Barren lands	0	0	8	10	0	0	0	1	114	4	0
	Desert	0	0	0	0	0	0	0	0	0	1	0
	Ice	0	0	0	0	0	0	0	0	0	0	2
2000	Forest	22	0	5	1	0	0	0	0	0	0	0
	Meadow steppe	0	3	0	1	0	0	0	0	0	0	0
	Real steppe	1	0	151	14	1	0	0	1	16	0	0
	Desert steppe	0	1	5	39	0	0	0	0	15	0	0
	Cropland	0	0	0	0	6	0	0	0	0	0	0
	Water	0	1	1	0	0	17	0	0	0	0	0
	Built area	0	0	0	0	0	0	2	0	0	0	0
	Sand	0	0	0	0	0	0	0	4	1	0	0
	Barren lands	0	0	1	6	0	0	0	0	100	0	0
	Desert	0	0	0	0	0	0	0	0	0	3	0
	Ice	0	0	0	0	0	0	0	0	0	0	2
2010	Forest	70	0	5	0	0	0	0	0	0	0	0
	Meadow steppe	3	20	3	0	0	1	0	0	2	0	0
	Real steppe	1	0	36	3	0	0	0	0	1	0	0
	Desert steppe	0	1	9	28	0	0	0	0	6	0	1
	Cropland	0	0	1	0	45	0	0	0	0	0	0
	Water	0	0	0	1	0	42	0	0	0	0	0
	Built area	0	0	12	3	0	0	20	0	2	0	0
	Sand	0	0	0	0	0	0	0	11	6	0	0
	Barren lands	0	0	0	1	0	0	0	0	50	0	0
	Desert	0	0	0	0	0	0	0	2	2	4	0
	Ice	0	0	0	1	0	1	0	0	5	0	3
2020	Forest	62	1	12	0	0	0	0	0	0	0	0
	Meadow steppe	2	24	2	0	0	1	0	0	0	0	0
	Real steppe	0	1	37	2	0	0	0	0	0	0	0
	Desert steppe	1	2	20	20	0	0	0	0	1	0	0
	Cropland	0	0	3	1	48	0	0	0	0	0	0
	Water	0	1	0	0	0	40	0	0	1	0	0
	Built area	0	0	4	3	0	0	30	0	0	0	0
	Sand	0	0	0	2	0	0	0	14	1	0	0
	Barren lands	0	0	0	3	0	0	0	2	45	0	0
	Desert	0	0	0	0	0	0	0	0	2	5	0
	Ice	0	0	0	3	0	0	0	0	2	0	4

20496060, 2022, 2, Downloaded from https://rmets.onlinelibrary.wiley.com/doi/10.1002/gdj3.149 by Curtin University Library, Wiley Online Library on [06/02/2023]. See the Terms and Conditions (https://onlinelibrary.wiley.com/terms-and-conditions) on Wiley Online Library for rules of use; OA articles are governed by the applicable Creative Commons License

TABLE 5 Producer accuracies, user accuracies, omission errors and commission errors of the land cover data

Year	Land cover type	Producer accuracies (%)	Omission errors (%)	User accuracies (%)	Commission errors (%)
1990	Forest	85.11	14.89	100.00	0.00
	Meadow steppe	85.71	14.29	54.55	45.45
	Real steppe	88.14	11.86	83.20	16.80
	Desert steppe	77.33	22.67	75.32	24.68
	Cropland	100.00	0.00	75.00	25.00
	Water	90.91	9.09	100.00	0.00
	Built area	62.50	37.50	100.00	0.00
	Sand	100.00	0.00	60.00	40.00
	Barren lands	83.21	16.79	92.68	7.32
	Desert	100.00	0.00	14.29	85.71
	Ice	100.00	0.00	100.00	0.00
2000	Forest	78.57	21.43	95.65	4.35
	Meadow steppe	75.00	25.00	60.00	40.00
	Real steppe	82.07	17.93	92.64	7.36
	Desert steppe	65.00	35.00	63.93	36.07
	Cropland	100.00	0.00	85.71	14.29
	Water	89.47	10.53	100.00	0.00
	Built area	100.00	0.00	100.00	0.00
	Sand	80.00	20.00	80.00	20.00
	Barren lands	93.46	6.54	75.76	24.24
	Desert	100.00	0.00	100.00	0.00
	Ice	100.00	0.00	100.00	0.00
2010	Forest	93.33	6.67	94.59	5.41
	Meadow steppe	68.97	31.03	95.24	4.76
	Real steppe	87.80	12.20	54.55	45.45
	Desert steppe	62.22	37.78	75.68	24.32
	Cropland	97.83	2.17	100.00	0.00
	Water	97.67	2.33	95.45	4.55
	Built area	54.05	45.95	100.00	0.00
	Sand	64.71	35.29	84.62	15.38
	Barren lands	98.04	1.96	67.57	32.43
	Desert	50.00	50.00	100.00	0.00
	Ice	30.00	70.00	75.00	25.00
2020	Forest	82.67	17.33	95.38	4.62
	Meadow steppe	82.76	17.24	82.76	17.24
	Real steppe	92.50	7.50	47.44	52.56
	Desert steppe	45.45	54.55	58.82	41.18
	Cropland	92.31	7.69	100.00	0.00
	Water	95.24	4.76	97.56	2.44
	Built area	81.08	18.92	100.00	0.00
	Sand	82.35	17.65	87.50	12.50
	Barren lands	90.00	10.00	86.54	13.46
	Desert	71.43	28.57	100.00	0.00
	Ice	44.44	55.56	100.00	0.00

20496060, 2022, 2, Downloaded from https://rmets.onlinelibrary.wiley.com/doi/10.1002/gdj3.149 by Curtin University Library, Wiley Online Library on [06/02/2023]. See the Terms and Conditions (https://onlinelibrary.wiley.com/terms-and-conditions) on Wiley Online Library for rules of use; OA articles are governed by the applicable Creative Commons License

the MP, the reasonable control of livestock husbandry in Mongolia, and other related studies.

6 | CONCLUSION

Based on the object-oriented remote sensing interpretation method, this study obtained refined land cover data for Mongolia with a 30-m resolution for the years 1990, 2000, 2010 and 2020 for the first time. The overall classification accuracies of the resulting land cover data for 1990, 2000, 2010 and 2020 were 82.26%, 82.77%, 92.34% and 81.84%, respectively. This study finds that land cover has a gradual zonal change. Land cover types from south to north are forest, real steppe, desert steppe and barren land. Among them, barren land, real steppe, desert steppe and forest have consistently been the four major land cover types. The sum of the areas under meadow steppe, water, sand, desert, cropland, built area, ice and snow has always been less than 6% of Mongolia's total land area. Since the last 30 years, barren land area, as a whole, has been presenting a decreasing trend, with a trend of southward reduction. Overall, real steppe presents a wavelike decreasing trend, and desert steppe shows a fluctuating increasing trend. Forest has consistently been relatively stable with no obvious changes in spatial distribution. The area under cropland has shown a continuously decreasing trend, while the built area has increased. This dataset can provide fundamental scientific data support for sustainable development in Mongolia. Further, the method used in this study can be used for land cover monitoring in the whole MP and even in other large areas of the world.

ACKNOWLEDGEMENTS

We are grateful to the members of the research team in the Institute of Geographic Sciences and Natural Resources Research, Chinese Academy of Sciences for the remote sensing interpretation of Mongolian land cover, and to the National University of Mongolia and Geography & Geoecology Institute at the Mongolian Academy of Sciences for their field work support. We want to thank the editor of this journal and the anonymous reviewers during the revision process.

OPEN PRACTICES STATEMNET

This article has earned an Open Data badge for making publicly available the digitally shareable data necessary to reproduce the reported results. The data are available at https://doi.org/10.6084/m9.figshare.14390912.v1. Learn more about the Open Practices badges from the Center for OpenScience: https://osf.io/tvyxz/wiki.

ORCID

Haishuo Wei https://orcid.org/0000-0002-0165-7771

REFERENCES

Asigang (2017) *Nearly 80% of land in Mongolia is suffering from desertification of varying degrees*. People's Daily, Available from: http://world.people.com.cn/n1/2017/0617/c1002-29345905.html

Baltsavias, E.P. (2004) Object extraction and revision by image analysis using existing geodata and knowledge: current status and steps towards operational systems. *ISPRS Journal of Photogrammetry and Remote Sensing*, 58(3–4), 129–151. https://doi.org/10.1016/j.isprsjprs.2003.09.002

Bao, G., Bao, Y.H., Tan, Z.H., Zhou, Y. & Shiirev, A. (2013) Vegetation cover changes in Mongolian plateau and its response to seasonal climate changes in recent 10 years. *Scientia Geographica Sinica*, 33(5), 613–621. https://doi.org/10.13249/j.cnki.sgs.2013.05.016

Batjargal, Z. (1997) Desertification in Mongolia. *Rala Report*, 200, 107–113.

Bayarkhuu. (2013) *Status of domestic timber production: Export and import dynamics in Mongolia*. Beijing Forestry University Master thesis.

Buren, G. (2011) *Research on current status, causes and prospect of desertification in Mongolia*. Inner Mongolia University Master thesis. doi: https://doi.org/10.7666/d.y1888732

Buyan-Erdene, J., Chinsu, L., Ishgaldan, B., Jamsran, R. & Khaulenbek, A. (2019) Applying a support vector model to assess land cover changes in the Uvs Lake Basin ecoregion in Mongolia. *Information Processing in Agriculture*, 6(1), 158–169. https://doi.org/10.1016/j.inpa.2018.07.007

Cao, X.M., Wang, J.L. & Feng, Y.M. (2016) An improvement of the Ts-NDVI space drought monitoring method and its applications in the Mongolian plateau with MODIS, 2000–2012. *Arabian Journal of Geosciences*, 9(6), 1–14. https://doi.org/10.1007/s12517-016-2451-5

Chen, J., Chen, J., Liao, A.P., Cao, X., Chen, L.J., Chen, X.H. et al. (2015) Global land cover mapping at 30 m resolution: A POK-based operational approach. *ISPRS Journal of Photogrammetry & Remote Sensing*, 103, 7–27.

Dai, Q. (2013) The land system reform of China viewed from Mongolia land Privatization. *Journal of Comparative Law*, 26(6), 146–158.

Foody, G.M. (2002) Status of land cover classification accuracy assessment. *Remote Sensing of Environment*, 80, 185–201. https://doi.org/10.1016/S0034-4257(01)00295-4

Gao, B.C. (1996) NDWI-A normalized difference water index for remote sensing of vegetation liquid water from space. *Remote Sensing of Environment*, 58(3), 257–266. https://doi.org/10.1016/s0034-4257(96)00067-3

Green, K. (2009) *Assessing the Accuracy of Remotely Sensed Data: Principles and Practices*, 2nd edition. Boca Raton, FL, USA: CRC Press/Taylor & Francis.

Hu, R.M., Wei, M., Yang, C.B. & He, J.B. (2012) Taking SPOT5 remote sensing data for example to compare pixel- based and object-oriented classification. *Remote Sensing Technology and Application*, 27(3), 366–371. https://doi.org/10.11873/j.issn.1004-0323.2012.3.366

Kearney, M.S., Townshend, J.R.G. & Rogers, A.S. (1995) *Developing a model for determining coastal marsh "health"*. Third Thematic

20496060, 2022, 2, Downloaded from https://rmets.onlinelibrary.wiley.com/doi/10.1002/gdj3.149 by Curtin University Library, Wiley Online Library on [06/02/2023]. See the Terms and Conditions (https://onlinelibrary.wiley.com/terms-and-conditions) on Wiley Online Library for rules of use; OA articles are governed by the applicable Creative Commons License

Conference on Remote Sensing for Marine and Coastal Environments, 527-537. Seattle, Washington.

Lamchin, M., Lee, J.Y., Lee, W.K., Lee, E.J., Kim, M., Lim, C.H. et al. (2016) Assessment of land cover change and desertification using remote sensing technology in a local region of Mongolia. *Advances in Space Research*, 57(1), 64–77. https://doi.org/10.1016/j.asr.2015.10.006

Ma, Y.Y., Zhang, C.X., Zhang, J.C., Xie, G.D. & Zhang, L.M. (2015) Research on object-oriented classification method assisted with NDVI/DEM in extracting cassava: taking wuming county for example. *Geography and Geo-Information Science*, 31(1), 49–53. https://doi.org/10.3969/j.issn.1672-0504.2015.01.011

Mengistie, K., Thomas, S., Demel, T. & Thomas, K. (2013) Land use/land cover change analysis using object-based classification approach in Munessa-Shashemene landscape of the Ethiopian highlands. *Remote Sensing*, 5, 2411–2435. https://doi.org/10.3390/rs5052411

Mongolian statistical information service. Available from: www.1212.mn

Ren, C.S., Ye, H.C., Cui, B. & Huang, W.J. (2017) Acreage estimation of mango orchards using object-oriented classification and remote sensing. *Resources Science*, 39(8), 1584–1591. https://doi.org/10.18402/resci.2017.08.14

Shi, H.D., Zhou, X.Y., Meng, F.H. & Bai, H.M. (2013) Mongolia and inner Mongolia LUCC regional differentiation over the past 30 years. *Journal of Geo-Information Science*, 15(5), 719–725. https://doi.org/10.3724/SP.J.1047.2013.00719

Tian, J., Wang, J.L., Li, Y.F., Zhou, Y.J., Guo, H.H. & Zhu, J.X. (2014) Land cover classification in Mongolian plateau based on decision tree method: a case study in Tov Province, Mongolia. *Journal of Geo-Information Science*, 3, 460–469. https://doi.org/10.3724/SP.J.1047.2014.00460

Uno, I.Z., Wang, M., Chiba, M., Chun, Y.S., Gong, S.L., Hara, Y. et al. (2006) Dust model intercomparison (DMIP) study over Asia: Overview. *Journal of Geophysical Research*, 111(2), 212–213. https://doi.org/10.1029/12005JD006575

Unurbaatar, B. & Caoligeer, Y.H. (2014) *The Spatial and Temporal Changes of Desertification in the Mongolian Plateau from 2000-2010*. In Proceedings of the Risk Analysis and Crisis Response in Information Technology-China Disaster Prevention Association Risk Analysis Professional Committee Annual Meeting, China Disaster Prevention Association Risk Analysis Professional Committee. Beijing, China.

Wang, J.L., Cheng, K., Liu, Q., Zhu, J.X., Altansukh, O., Davaadorj, D. et al. (2019) Land cover patterns in Mongolia and their spatio-temporal changes from 1990 to 2010. *Arabian Journal of Geosciences*, 12, 778. https://doi.org/10.1007/s12517-019-4893-z

Wang, J.L., Cheng, K., Zhu, J.X. & Liu, Q. (2018) Development and pattern analysis of Mongolian land cover data products with 30 meters resolution. *Journal of GeoInformation Science*, 20(9), 1263–1273. https://doi.org/10.12082/dqxxkx.2018.180153

Wang, J.L., Wei, H.S., Cheng, K., Altansukh, O., Davaadorj, D., Li, P.F. et al. (2020) Spatio-temporal pattern of land degradation from 1990 to 2015 in Mongolia. *Environmental Development*, 34, 100497, https://doi.org/10.1016/j.envdev.2020.100497

Wang, J.L., Wei, H.S., Cheng, K., Li, G., Altansukh, O., Davaadorj, D. et al. (2019) Spatio-temporal pattern of land degradation along the China-Mongolia railway (Mongolia). *Sustainability*, 11, 2705. https://doi.org/10.3390/su11092705

Wang, J.L., Wei, H.S., Cheng, K., Shao, Y.T., Yao, J.Y., Wu, Y.X. et al. (2021) *An updatable dataset revealing changes in land cover types in Mongolia*. figshare. Available from: https://doi.org/https://doi.org/10.6084/m9.figshare.14390912.v1

Wei, L.S. (2015) Analysis of reasons, characteristics and results of Mongolia's political and economic transformation. *Science Economy Society*, 1, 89–92. doi: CNKI:SUN:KJSH.0.2015-01-018.

Wei, Y.J., Zhen, L., Liu, X.L. & Ochirbat, B. (2008) Land use change and its driving factors in Mongolia from 1992 to 2005. *Chinese Journal of Applied Ecology*, 9, 1995–2002. https://doi.org/10.13287/j.1001-9332.2008.0366

Yue, D.Y., Du, J., Liu, J.Y., Guo, J.J., Zhang, J.J. & Ma, J.H. (2011) Spatio-temporal analysis of ecological carrying capacity in Jinghe Watershed based on Remote sensing and Transfer Matrix. *Acta Ecologica Sinica*, 9, 2550–2558. doi: CNKI:SUN:STXB.0.2011-09-026.

Zhang, X.Y., Gong, S.L., Zhao, T.L., Arimoto, R., Wang, Y.Q. & Zhou, Z.L. (2003) Sources of Asian dust and role of climate change versus desertification in Asian dust emission. Geography. *Geophysical Research Letters*, 30(2), 65–72. https://doi.org/10.1029/2003GL018206

Zhang, X.T., Tan, Q.L., Tu, T.Q., Dong, X.F. & Li, Y. (2019) Evaluation of ecological carrying capacity along "grassland road" in Mongolia using MODIS satellite data. *Geomatics & Spatial Information Technology*, 42(9), 64–67. doi: CNKI:SUN:DBCH.0.2019-09-019.

Zhang, Y.J. (2016) *Analysis on the characteristics and changes of Land desertification in Mongolian Plateau*. The thesis of Master, University of Chinese Academy of Sciences.

Zheng, W. & Zeng, Z.Y. (2004) A review on methods of atmospheric correction for remote sensing images. *Remote Sensing Information*, 4, 66–70. https://doi.org/10.3969/j.issn.1000-3177.2004.04.019

Zhou, X.Y., Shi, H.D. & Wang, X.R. (2014) Impact of climate change and human activities on vegetation coverage in the Mongolian plateau. *Arid Zone Research*, 4, 604–610. https://doi.org/10.13866/j.azr.2014.04.04

Zhuo, Y. (2007) *The ration remote sensing method study of desertification of Mongolia Plateau based on MODIS data*. Inner Mongolia Normal University Master thesis. https://doi.org/10.7666/d.y1173638

How to cite this article: Wang, J., Wei, H., Cheng, K., Ochir, A., Shao, Y., Yao, J., et al (2022) Updatable dataset revealing decade changes in land cover types in Mongolia. *Geoscience Data Journal*, 9, 341–354. Available from: https://doi.org/10.1002/gdj3.149

20496060, 2022, 2, Downloaded from https://rmets.onlinelibrary.wiley.com/doi/10.1002/gdj3.149 by Curtin University Library, Wiley Online Library on [06/02/2023]. See the Terms and Conditions (https://onlinelibrary.wiley.com/terms-and-conditions) on Wiley Online Library for rules of use; OA articles are governed by the applicable Creative Commons License